UNITED NATIONS EDUCATIONAL, SCIENTIFIC AND CULTURAL ORGANIZATION
INTERNATIONAL ATOMIC ENERGY AGENCY
INTERNATIONAL CENTRE FOR THEORETICAL PHYSICS
I.C.T.P., P.O. BOX 586, 34100 TRIESTE, ITALY, CABLE: CENTRATOM TRIESTE

H4.SMR/942-7

Third Workshop on
3D Modelling of Seismic Waves Generation
Propagation and their Inversion

4 - 15 November 1996

Characteristics of Surface Waves Generated by Events and Near the Chinese Nuclear Test Site

A. Levshin and M. Ritzwoller

Dept. of Physics
University of Colorado
Boulder, CO, U.S.A.

Geophys. J. Int. (1995) **123**, 131–148

Characteristics of surface waves generated by events on and near the Chinese nuclear test site

Anatoli L. Levshin and Michael H. Ritzwoller
Department of Physics, University of Colorado, Boulder, CO 80309-0583, USA

Accepted 1995 April 10. Received 1995 March 31; in original form 1994 November 21

SUMMARY

Our goal is to characterize surface waves at intermediate periods (5–30 s) generated by nuclear explosions and natural earthquakes occurring in and around the Chinese nuclear test site at Lop Nor observed at epicentral distances between 10° and 20°. We present observations of Rayleigh- and Love-wave group velocities, spectral amplitudes and polarizations for eight nuclear explosions and nine earthquakes recorded at IRIS and GEOSCOPE broad-band digital stations and at the Kirghiz Telemetered Seismic Network (KNET). The wave paths studied cross complex geological regimes. Waveforms are extremely complicated, yet observations made with frequency–time analysis are robust and repeatable.

(1) Group velocity and spectral amplitude measurements vary strongly across the studied region, but display understandable systematics related to known tectonic features.

(2) Both group velocity and spectral amplitude measurements across the KNET array are generally similar at periods above 10 s, but differences are striking at shorter periods. Stacking methods dependent on waveform coherence across the network should only succeed at periods above 10 s for this large-scale array.

(3) Group velocity measurements for earthquakes and nuclear explosions that share a common wave path agree well, but spectral amplitudes differ appreciably, especially for Rayleigh waves. Typically, earthquake spectra are enriched in longer periods (12–20 s) relative to explosion spectra for events of the same magnitude.

(4) Higher modes are observed on frequency–time diagrams for Rayleigh waves generated by earthquakes, but are not observed for explosions.

(5) Multipathing is observed in both frequency–time diagrams and polarization analyses, but, again, is qualitatively understandable in terms of known structural features. In particular, the channelling of Love waves by the Tarim Basin is documented.

(6) Large-amplitude Love waves are generated by nuclear explosions at Lop Nor, indicative of significant tectonic release.

We discuss the relevance of the differences in spectral amplitudes between earthquakes and explosions and of the appearance of higher modes on earthquake frequency–time diagrams to the problem of discriminating nuclear explosions from earthquakes.

Key words: Asia, Love waves, nuclear explosions, Rayleigh waves, seismic-wave propagation.

1 INTRODUCTION

Development of efficient and robust methods for detecting and identifying small underground nuclear explosions on the basis of their seismic signatures is one of the great challenges of modern seismology. The well known and generally most successful seismic discriminant between explosions and shallow earthquakes is based on the difference between two magnitudes (m_b and M_s) determined from the amplitudes of P waves and Rayleigh surface waves, respectively (Press, Dewart & Gilman 1963; Dahlmann & Israelson 1977). Unfortunately, this discriminant fails when events become too weak for measuring

amplitudes of surface waves by standard methods (at 20 s period) and breaks down as events become increasingly smaller (e.g. Lieberman & Pomeroy 1969).

To overcome these fundamental difficulties of discrimination, improved methods have emerged. These have included maximum amplitude ratios of certain body waves (short period) and surface waves (longer period) in certain restricted frequency bands (e.g. Pomeroy, Best & McEvilly 1982; Taylor *et al.* 1989; Baumgardt & Young 1990; Hedlin, Minster & Orcutt 1990; Kennett 1993; Woods, Kedar & Helmberger 1993; Wuster 1993), body-wave spectral peaks and slopes (e.g. Bakun & Johnson 1970; Murphy & Bennett 1982; Evernden, Archambeau & Cranswick 1984; Stevens & Day 1985; Stevens 1986; Chael 1988; Taylor, Sherman & Denny 1988), 'Master Event' correlation analysis (e.g. Joswig & Schulte-Theis 1993) and the analysis of sonograms (e.g. Harjes & Joswig 1985; Joswig 1990). Each of these methods suffers problems.

To complement these methods, we wish to investigate in more detail the application to discrimination of intermediate-period (5–30 s) surface-wave spectral characteristics, particularly in the complex tectonic environment of central Asia. In order to do so, it is necessary to develop a deeper insight into the differences between surface-wave patterns created by earthquakes and explosions at the regional epicentral distances at which seismic monitoring may readily be performed. Surface waves in the range of periods between several seconds and several tens of seconds are one of the most natural subjects for such scrutiny, as the surface-wave excitation function is very sensitive to the depth of source, as well as to its temporal and spatial sizes and geometry.

To make this study possible it is necessary to have access to broad-band digital records of seismic waves generated by earthquakes and explosions in the same region. A natural choice for such a region is the Xinjiang Province of China, in and around the Chinese nuclear test site near Lake Lop Nor. First, this region is seismically quite active (e.g. Gao & Richards 1994). Thus, we can compare surface-wave patterns from both earthquakes and nuclear explosions occurring at nearly the same location. Second, the recent deployments by the USGS and IRIS of digital broad-band seismic stations and the regional Kirghiz Telemetered Seismic Network (KNET) in central Asia have made available for analysis an impressive set of high-quality broad-band data. In this paper we will discuss the systematics of surface waves generated by explosions and earthquakes in and around Lop Nor which propagate at regional distances across the complex tectonic regimes of central and southern Asia. This study is part of a more general work on the regional characterization of surface waves propagating across central Asia.

Our goal here is to address the following questions, which are aimed at determining if intermediate-period (5–30 s) surface-wave data at regional distances may be relevant to problems of discrimination and at evaluating possible caveats when using such data in regions set in complex tectonic environments (such as the spatial variability of wave characteristics, multipathing, tectonic release, etc.).

(1) What is the variability across the studied region of intermediate period (5–30 s) Rayleigh- and Love-wave group velocities and spectral amplitudes for earthquakes and nuclear explosions that occur at Lop Nor?

(2) How do measurements of these quantities vary for a single event across the KNET array?

(3) How do these measurements across the studied region compare between earthquakes and nuclear explosions?

(4) Is there indication that measurements such as these hold promise as a potential discriminant?

(5) What are the impacts of factors that potentially complicate waveforms, in particular multipathing and tectonic release from nuclear explosions?

Section 2 of the paper presents the relevant observations which are then discussed in Section 3. As we shall see, Rayleigh- and Love-wave spectral amplitudes differ substantially between earthquakes and nuclear explosions occurring at Lop Nor. As

Table 1. List of selected events at and around Lop Nor test site.

n	Latitude	Longitude	Depth	Date	Jday	Time	M_b	M_s	Type
1[1]	41.75	88.47	0	09/29/1988	273	07:00:03.1	4.3	-	EXPLOSION
2	42.02	89.29	33	11/15/1988	320	16:56:46.2	5.0	4.3	EARTHQUAKE
3	42.07	90.58	10	01/05/1989	005	17:42:20.8	4.3	-	EARTHQUAKE
4	41.53	88.73	33	01/21/1990	021	07:53:31.9	4.6	-	EARTHQUAKE
5[2]	41.57	88.69	0	05/26/1990	146	07:59:57.8	5.4	-	EXPLOSION
6	41.56	88.77	0	08/16/1990	228	04:59:57.6	6.2	-	EXPLOSION
7	40.88	89.07	22	11/03/1990	307	17:25:13.8	5.1	4.1	EARTHQUAKE
8	42.70	87.22	32	06/06/1991	157	08:02:07.5	5.1	4.4	EARTHQUAKE
9	41.39	87.81	33	12/18/1991	352	13:44:04.1	4.4	-	EARTHQUAKE
10	41.60	88.81	0	05/21/1992	142	04:59:57.5	6.5	5.0	EXPLOSION
11[3]	41.76	88.39	0	09/25/1992	269	07:59:59.9	5.0	-	EXPLOSION
12	41.98	89.28	14	11/27/1992	332	16:09:09.1	5.3	4.8	EARTHQUAKE
13	42.90	87.04	33	04/14/1993	104	08:31:09.7	4.4	-	EARTHQUAKE
14	40.12	91.53	33	05/26/1993	146	14:11:12.4	4.4	-	EARTHQUAKE
15	41.67	88.69	0	10/05/1993	278	01:59:56.6	5.9	4.7	EXPLOSION
16	41.57	88.70	0	06/10/1994	161	06:25:58.0	5.7	-	EXPLOSION
17	41.55	89.07	0	10/07/1994	280	03:25:58.0	5.9	-	EXPLOSION

Notes: [1] Listed in the PDE as an earthquake at a depth of 33 km. [2] Listed in the PDE as an earthquake at a depth of 0 km. [3] Listed in the PDE as an earthquake at a depth of 10 km.

a consequence, we will argue that further systematic study of intermediate-period surface-wave characteristics is warranted, but there are a number of factors that complicate their use as a discriminant.

2 OBSERVATIONS

2.1 Data selection and processing

The epicentral region under study is limited by latitudes 40° N and 43° N and longitudes 87° E and 91° E. Records from IRIS/IDA stations AAK (Ala-Archa, Kirghizstan), ABKT (Alibek, Turkmenistan), GAR (Garm, Tadjikistan), TLY (Talaya, Russia); KNET stations (Harvey & Hansen 1994; Vernon 1994); the GEOSCOPE station HYB (Hyderabad, India); and the Chinese Digital Seismic Network (CDSN) stations LZH (Lanzhou), LSA (Lhasa, Tibet), BJI (Beijing), KMI (Kunming), WMQ (Urumqi) are used in the surface-wave analyses. These stations are situated between 1200 and 2800 km from Lop Nor. The single exception is WMQ which is only 260 km away from the test site. Because data from IRIS/IDA stations are available only from the middle of 1988, we studied events which occurred in this region from 1988 September through 1994 October. PDE bulletins for this time period list 17 events, eight of which are presumed nuclear explosions and nine are earthquakes (Table 1). Positions of stations and epicentres are shown in Fig. 1.

To analyse seismic records we used interactive techniques based on a frequency–time representation of seismic signals (Dziewonski, Bloch & Landisman 1969; Levshin, Pisarenko &

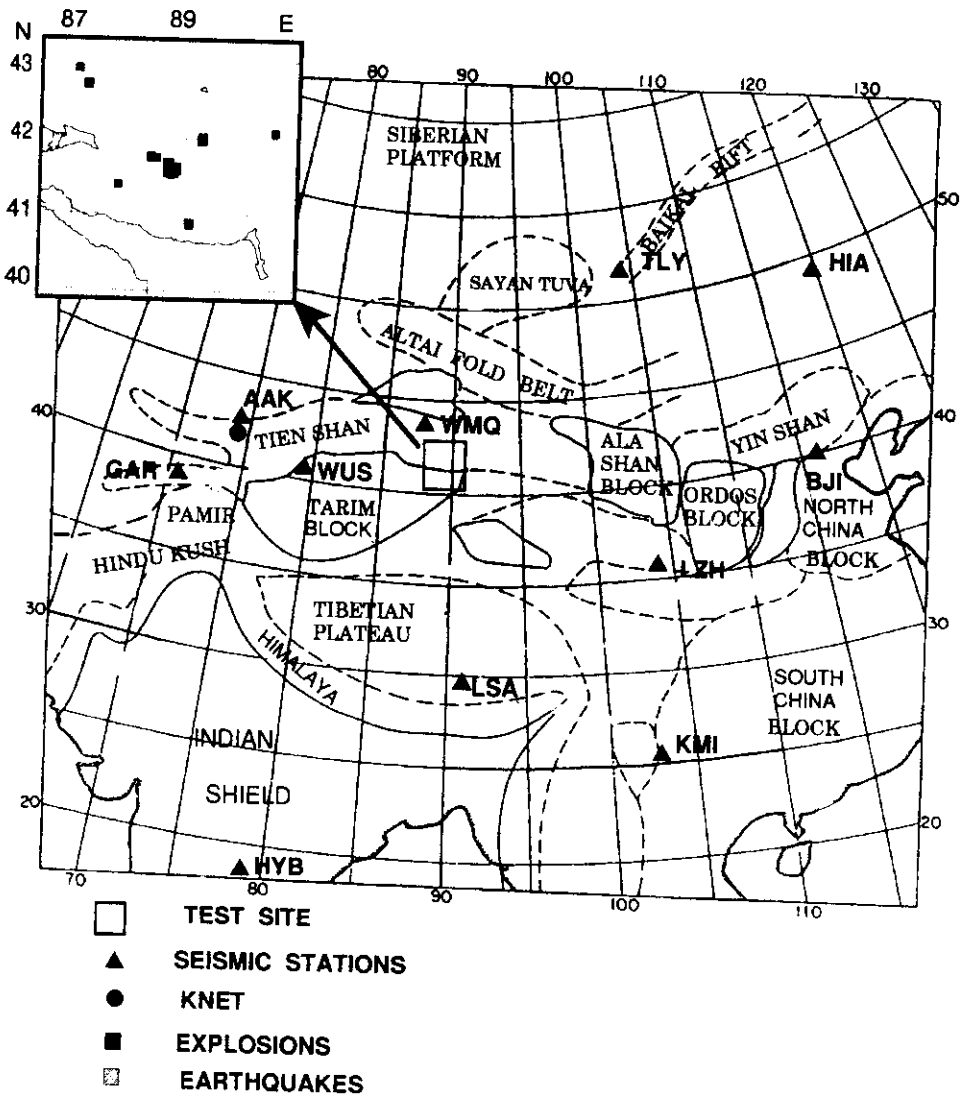

Figure 1. Tectonic scheme of the region (after Terman 1973; Sengor, Natal'in & Burtman 1993). The locations of the Chinese test site and seismic stations used in the study are shown. Station ABKT is outside the map at 39.9° N, 58.1° E. The locations of epicentres of selected events are shown on the detailed map of the Lop Nor area in the upper left corner.

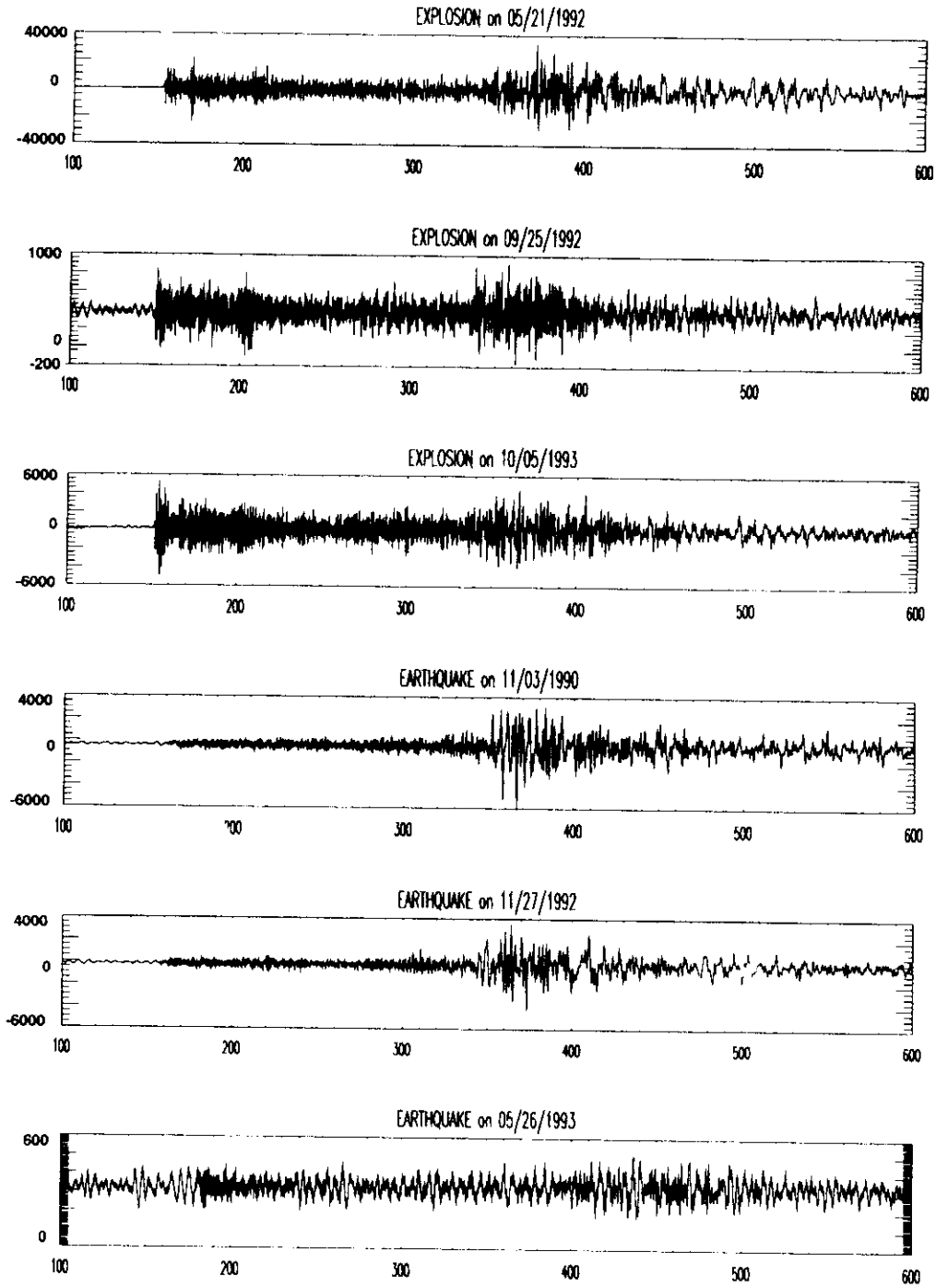

Figure 2. Comparison of broad-band seismograms for six events near Lop Nor recorded at AAK (vertical component). The three upper traces are records of nuclear explosions (yields are approximately 1 Mt, 10 kt and 60 kt), the three lower traces are records of earthquakes (m_b is 5.1, 5.3 and 4.4). Differences between records of large explosions and strong earthquakes are clearly seen.

Pogrebinsky 1972). Such a representation, often called the Gabor transform, is obtained in practice by passing an input record through a comb of narrow frequency–band Gaussian filters and presenting amplitudes of envelopes and instant phases of filter outputs as a 2-D complex function of time and frequency. When a three-component record is analysed the resulting representation is a complex vector function of the same variables. Details of the applied procedure for the frequency time analysis (FTAN) and its generalization for the frequency–time polarization analysis (FTPAN) of three-component records are given by Levshin and co-workers (Levshin *et al.* 1989; Levshin, Pisarenko & Pogrebinsky 1992;

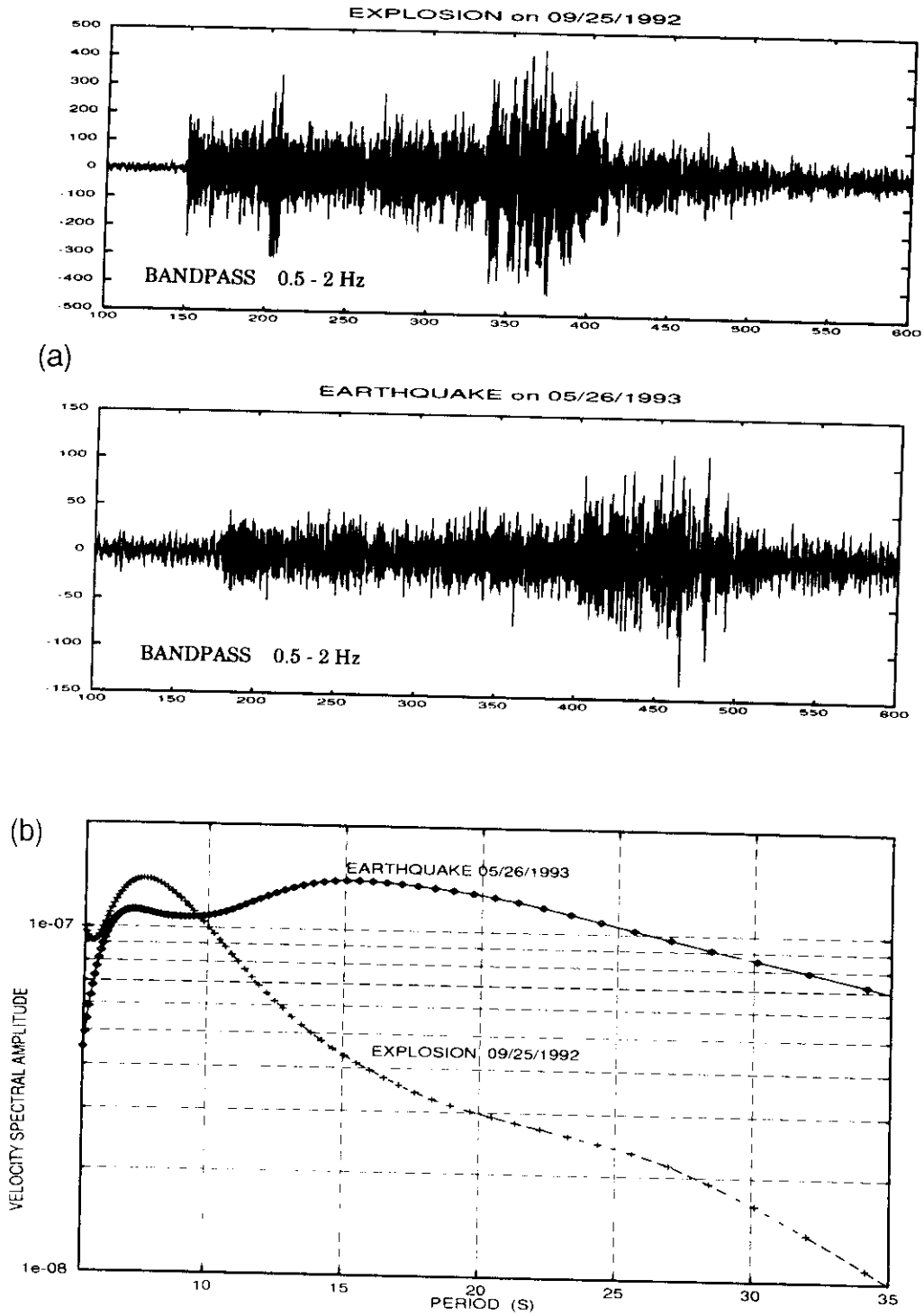

Figure 3. Comparison of narrow-band seismograms and extracted Rayleigh-wave spectra for relatively weak events recorded at AAK: an explosion on 1992 September 25 (10 kt) and an earthquake on 1993 May 26 ($m_b = 4.4$). (a) Seismograms are bandpassed in the range 0.5–2 Hz; no obvious differences are evident. (b) Spectra of Rayleigh-wave signals extracted from broad-band records (Fig. 2) are significantly different.

Levshin, Ritzwoller & Ratnikova 1994). These techniques are especially efficient for resolving complicated dispersive wave patterns caused by multipathing which are typical for the tectonic regime under study here.

To extract a desired signal from several high-amplitude patches on a FTAN amplitude diagram we used the technique of floating filtering (Cara 1973; Levshin *et al.* 1989). An interactively determined group velocity curve is used to obtain

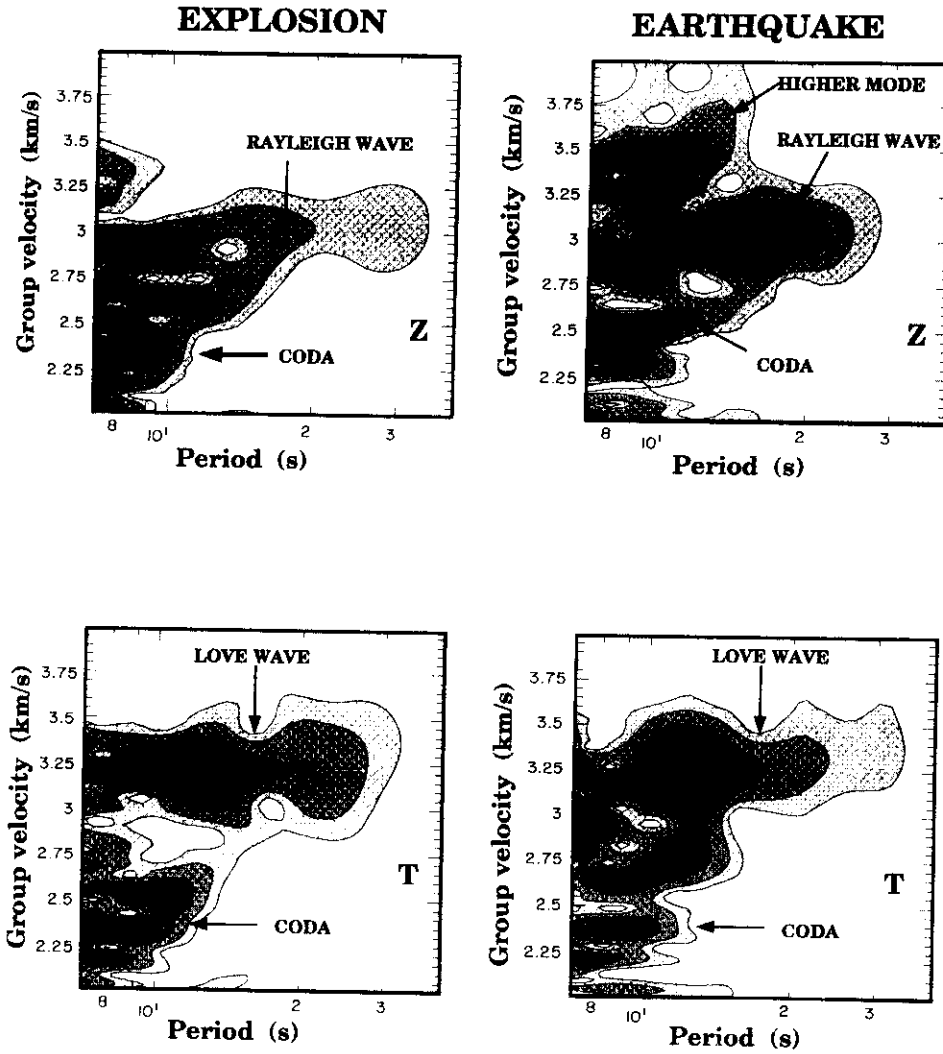

Figure 4. Frequency–time diagrams of vertical (Z) and transverse (T) components of the surface waves recorded at AAK for the explosion on 1992 May 21 and the earthquake on 1992 November 27 near Lop Nor. Surface waves from the earthquake are relatively more intense in the long-period part of the spectra.

a spectral phase correction which will compensate the effect of dispersion on the extracted signal. This phase correction, introduced into the input record's spectrum, contracts the desired signal into a temporarily limited function. As a result, it becomes possible to apply a tapering time window to extract the contracted signal from the transformed record and then to restore the cleaned signal by applying to its spectrum the same phase correction but with the opposite sign. This procedure has many features in common with the residual dispersion measurement technique of Dziewonski, Mills & Bloch (1972) and phase-matched filtering by Herrin & Goforth (1977) and Russell, Herrman & Hwang (1988). A characteristic feature of our procedure is that it is fully implemented in the framework of the frequency–time analysis without the use of any additional information about the medium or the signals. This approach makes the procedure of analysis internally consistent and straightforward and allows for the simultaneous determination of phase and group velocities, amplitude spectra and polarization parameters of different surface waves interfering in the time and frequency domains (fundamental and higher Rayleigh and Love waves, multiple arrivals) as can be seen in Fig. 4. Floating filtering has been applied here only in the range of periods between about 5 and 40 s. Measurements on the extracted signals are reliable only within this range and should not to be interpreted at shorter or longer periods.

2.2 Characterization of records and frequency–time diagrams

Typical broad-band records of explosions and earthquakes near Lop Nor recorded by AAK at an epicentral distance of about 1200 km are shown in Fig. 2. Fig. 2 demonstrates the striking difference in relative P-wave and surface-wave amplitudes among records of strong explosions (yield of approximately 1 Mt and 60 kt; first and third records) and earthquakes (magnitudes $m_b = 5.1$–5.3; fourth and fifth records). However, such drastic differences are not apparent between broad-band records of weaker events (10 kt explosion and an earthquake

with $m_b = 4.4$; the second and the sixth records in Fig. 2). These events differ in body-wave magnitude by about 0.5, but are comparable in the level of energy generated around 0.1 Hz and at lower frequencies. Narrow-band records of the same events (bandpass 0.5–2 Hz, Fig. 3a) are quite similar, posing even greater problems for discrimination. Thus, as source magnitude decreases and as epicentral distance increases, time-domain differences among records of earthquakes and explosions become less distinct. This is one of the problems for discriminants based on amplitude ratios, as discussed in Section 1.

The use of intermediate-period surface waves to provide added information of relevance to seismic discrimination is based on the analysis of frequency–time diagrams such as those shown in Fig. 4. Such diagrams in the range of periods between 5–8 and 30–40 s and in the range of group velocities between 1.5 and 4 km s^{-1} both for earthquakes and explosions look quite complicated, especially for paths crossing regions with high relief (e.g. to AAK, GAR). One can see in Fig. 4 very strong fundamental Rayleigh and Love surface waves on the vertical and tangential components, respectively, as well as higher mode and scattered energy (coda).

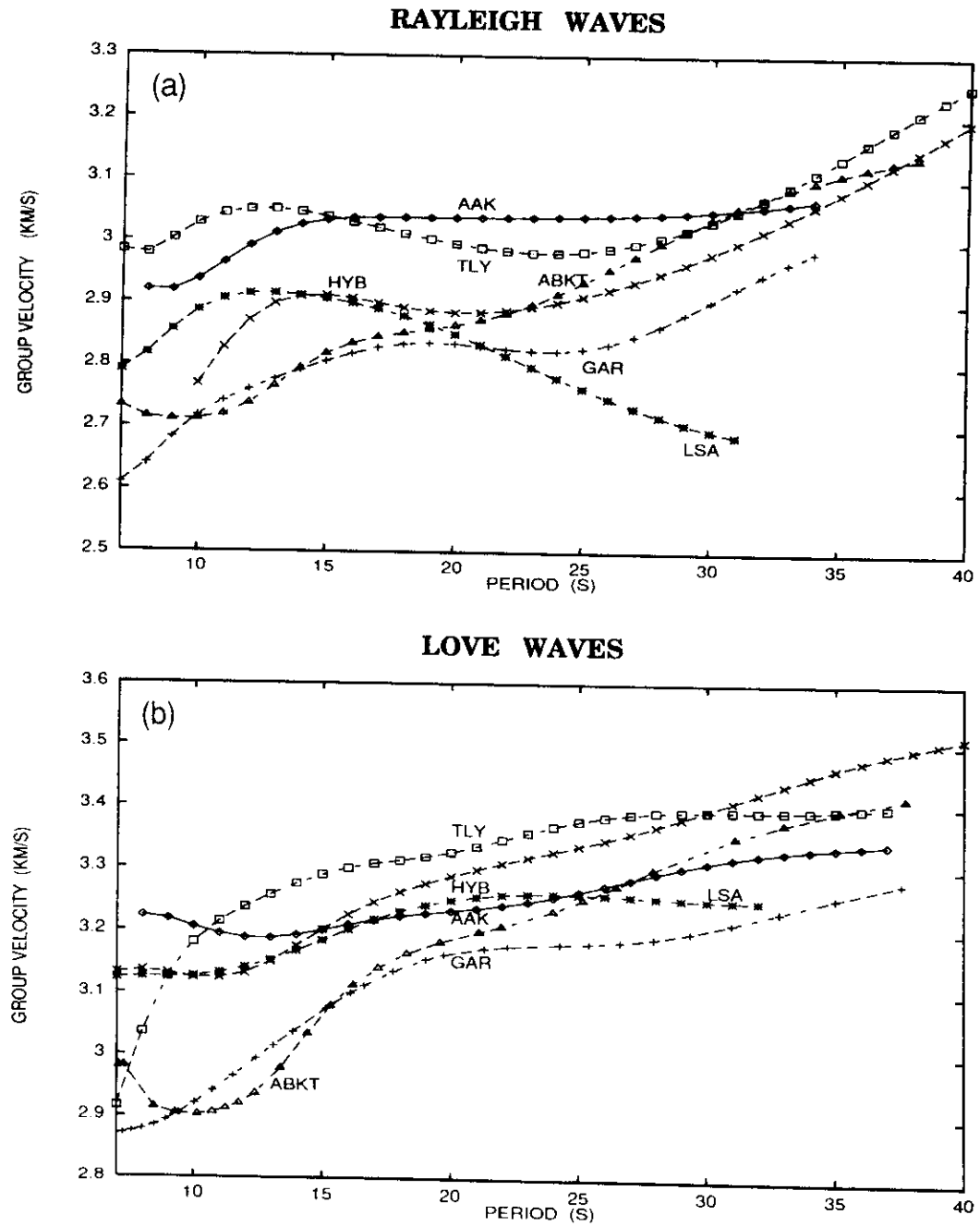

Figure 5. Variability of surface-wave group velocities from Lop Nor to selected stations: (a) Rayleigh waves, (b) Love waves.

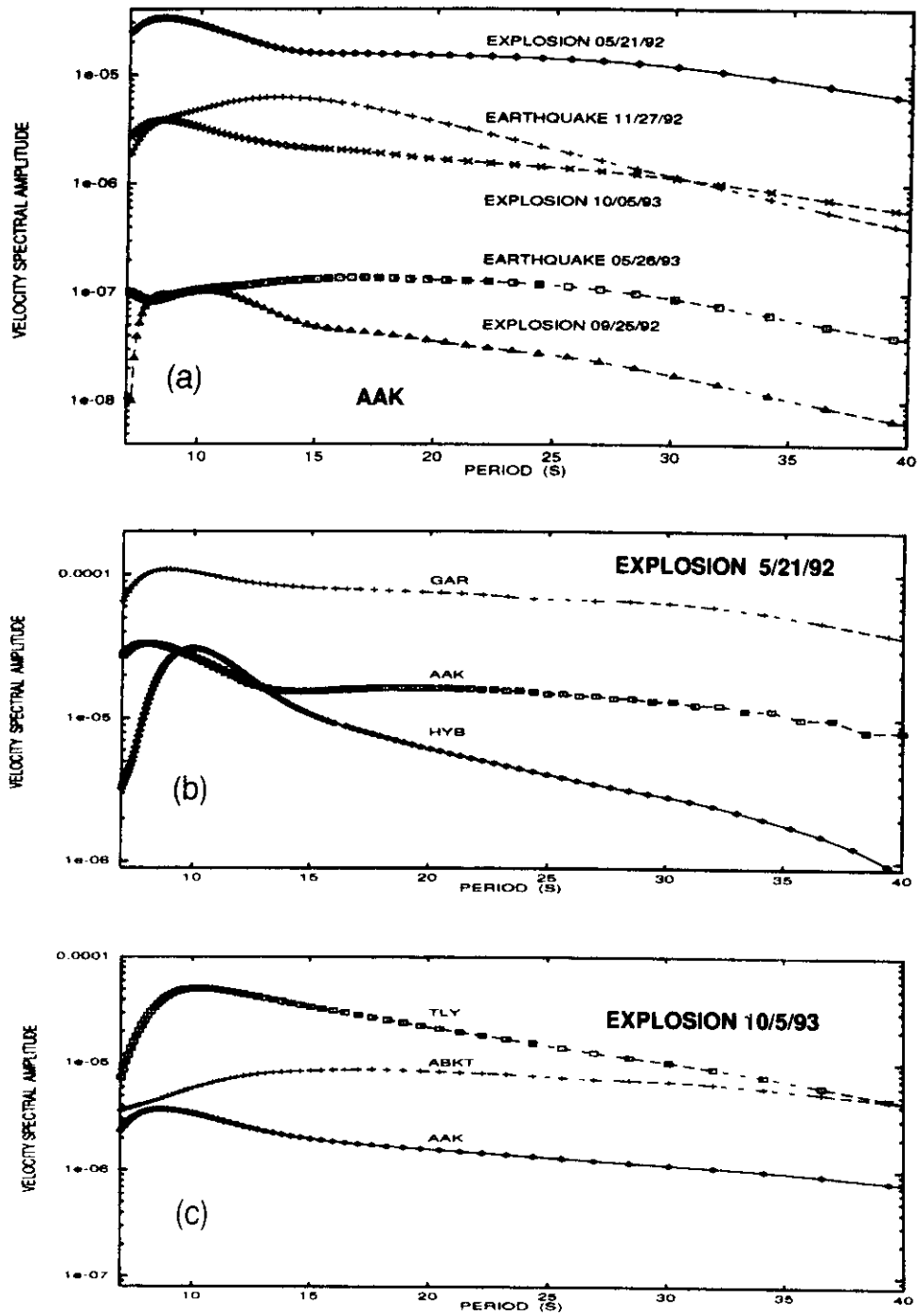

Figure 6. Similarities and differences in velocity amplitude spectra of Rayleigh waves for different events recorded at various stations. (a) AAK: three explosions and two earthquakes near Lop Nor. (b) GAR, AAK, HYB: the explosion of 1992 May 21; velocity amplitudes at AAK are observed amplitudes in metres per second; velocity amplitudes at GAR and HYB are observed amplitudes in metres per second times $10^{1.656\log(\Delta/\Delta_{AAK})}$, where Δ is the epicentral distance for the given station in degrees (Gutenberg 1945). (c) TLY, ABKT, AAK: the explosion on 1993 October 5; velocity amplitudes at AAK are observed amplitudes in metres per second; velocity amplitudes at TLY and ABKT are observed amplitudes in metres per second times the same factor as in (b).

Analyses of these diagrams reveal three principal observations. (1) As a rule, the Rayleigh and Love waves generated by earthquakes extend to longer periods than those generated by explosions of about the same magnitude m_b. This is especially true for the Rayleigh waves. This can be seen more clearly on spectral amplitude plots such as Fig. 3(b). (2) Higher modes of these waves are often seen well for earthquakes, but are less distinct on records of explosions. (3) The later parts of these

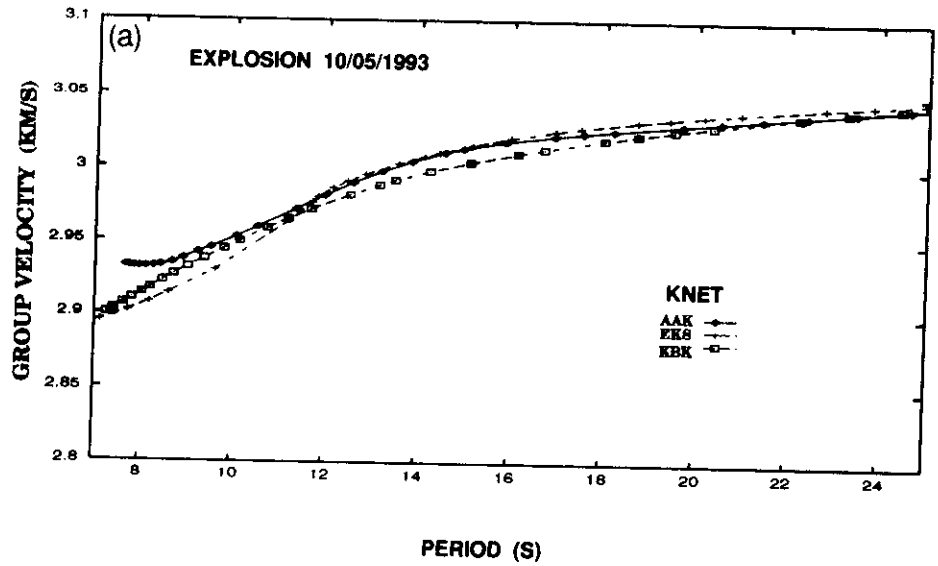

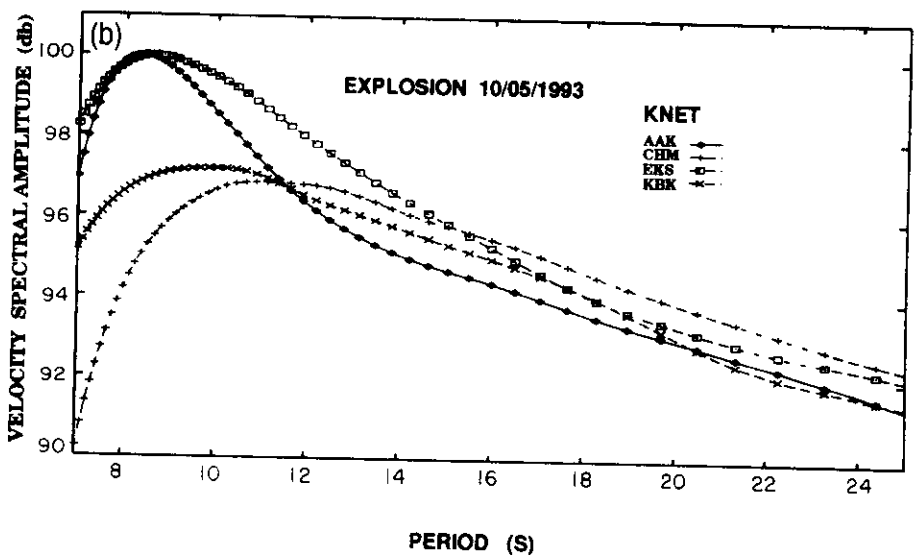

Figure 7. Group velocities and amplitude spectra of Rayleigh waves at several KNET stations for the explosion on 1992 May 21: (a) group velocity curves; (b) velocity amplitude spectra.

diagrams display very strong surface-wave codas, including several very distinct phases often with amplitudes comparable to direct surface waves. The frequency range of the coda is narrower than that of the direct surface waves, generally confined to periods below 15 s.

2.3 Surface-wave group velocities

Group velocity curves for Rayleigh and Love waves for a variety of paths from Lop Nor are shown on Figs 5(a) and (b), respectively. Significant differences in group velocities (up to 0.5–0.7 km s^{-1}) between different paths are apparent, not only at short periods but also at periods of 30 s and higher. The highest velocities are observed for paths to AAK and TLY, the lowest velocities for paths to GAR and, at long periods, to LSA. Low velocities at shorter periods (8–15 s) are observed for the path to ABKT. However, group velocity curves for a given station and the whole set of events near Lop Nor are very similar. The characteristics of group velocities across central Asia will be discussed elsewhere. Our main interest here is in spectral amplitudes.

2.4 Surface-wave amplitude spectra

Rayleigh-wave amplitude spectra extracted by means of floating filtering for various explosions recorded at the same station are quite similar in form and differ mainly in the DC level (Fig. 6a) which is dominantly controlled by moment. Velocity spectral amplitudes are presented on an absolute logarithmic scale. Amplitude spectra of the same explosion recorded at different stations usually display quite different spectral characteristics, such as peak periods and roll-offs, as Figs 6(b) and (c) show. These figures are intended to display the location of spectral peaks and spectral shapes.

Earthquakes produce a much greater variety of spectral shapes even for the same station (Fig. 6a), presumably due to source complexity. Typically, however, the maxima of earthquake surface-wave-amplitude spectra are at significantly longer periods than explosion spectral maxima, as can be seen in Figs 3(b), 4 and 6. This is true not only for large events, but also for small events such as the explosion on 1992 September 10 (10 kt) and the earthquake on 1993 May 26 ($m_b = 4.4$) mentioned above. Fig. 3(b) demonstrates the significance of the difference in position of the Rayleigh-wave spectral peaks for these two events: 10 s for the explosion and 17 s for the earthquake. Figs 7(a) and (b) show that surface waves for the same event recorded at different KNET stations (KNET's aperture is of the order 100 km) generally have very similar group velocity and spectral amplitude curves at periods longer than 8–10 s. At shorter periods, however, significant differences are observed.

2.5 Later arrivals

One of the most striking features of the surface-wave patterns which are observed at several stations for Lop Nor events is the presence of intense later arrivals with very low apparent group velocities. Their spectral amplitudes relative to the main surface-wave train are quite stable for all explosions but vary widely among the earthquakes. This is particularly well seen on records at the station GAR situated at a distance of 1600 km to the West of Lop Nor, near the border between the Tien Shan and Pamir Mountains. Fig. 8(a) presents frequency–time diagrams and the corresponding bandpassed seismograms for the transverse component of the surface waves at GAR for three events at Lop Nor: two earthquakes (1990 November 3 and 1990 January 21) and a nuclear test (1992 May 21). These records were obtained by rotating the horizontal components using the theoretical backazimuth for the great circle path linking Lop Nor to GAR.

For the earthquake on 1990 November 3 the dominant feature of the transverse component is an extremely slow strongly dispersed Love wave (middle panel, Fig. 8a). The same wave can be seen on records of the earthquake on 1990 January 21 (top panel, Fig. 8a) and the large nuclear explosion (bottom panel, Fig. 8a), but in these cases this wave is preceded by the faster and only slightly dispersive Love wave of comparable intensity. Group velocity curves for these two Love waves (numbered 1 and 2) and the Rayleigh wave for four different events recorded at GAR are shown in Fig. 8(b). Polarization analysis in Fig. 8(c) shows that the slow Love wave (L2) arrives at GAR 10°–15° to the south of the great circle linking Lop Nor to GAR. However, the 'normal' Rayleigh (R1) and Love (L1) waves arrive at GAR 15°–20° to the north of the same great circle. Frequency–time diagrams at GAR and other stations for another comparatively strong

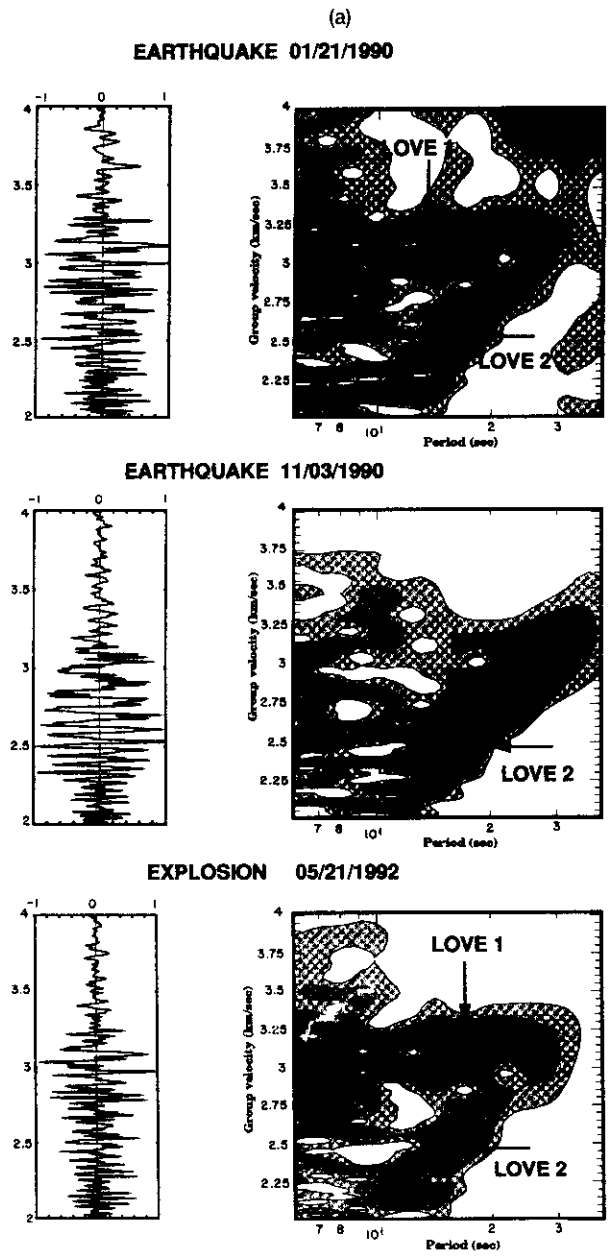

Figure 8. (a) Evidence of multipathing: bandpassed seismograms and frequency–time diagrams of the transverse component of the surface waves recorded at GAR for three events near Lop Nor. (b) Group velocity curves for these events. (c) Azimuthal deviations observed at GAR for different waves.

explosion on 1990 August 16 are very similar to those for an explosion of 1992 May 21.

2.6 Love waves generated by explosions

Large-amplitude Love waves generated by explosions are observed not only at GAR, but are also seen on records from practically all of the selected stations. Fig. 9(a) illustrates the strength of the transverse components from the explosion of 1992 May 21 at three KNET stations in comparison with the

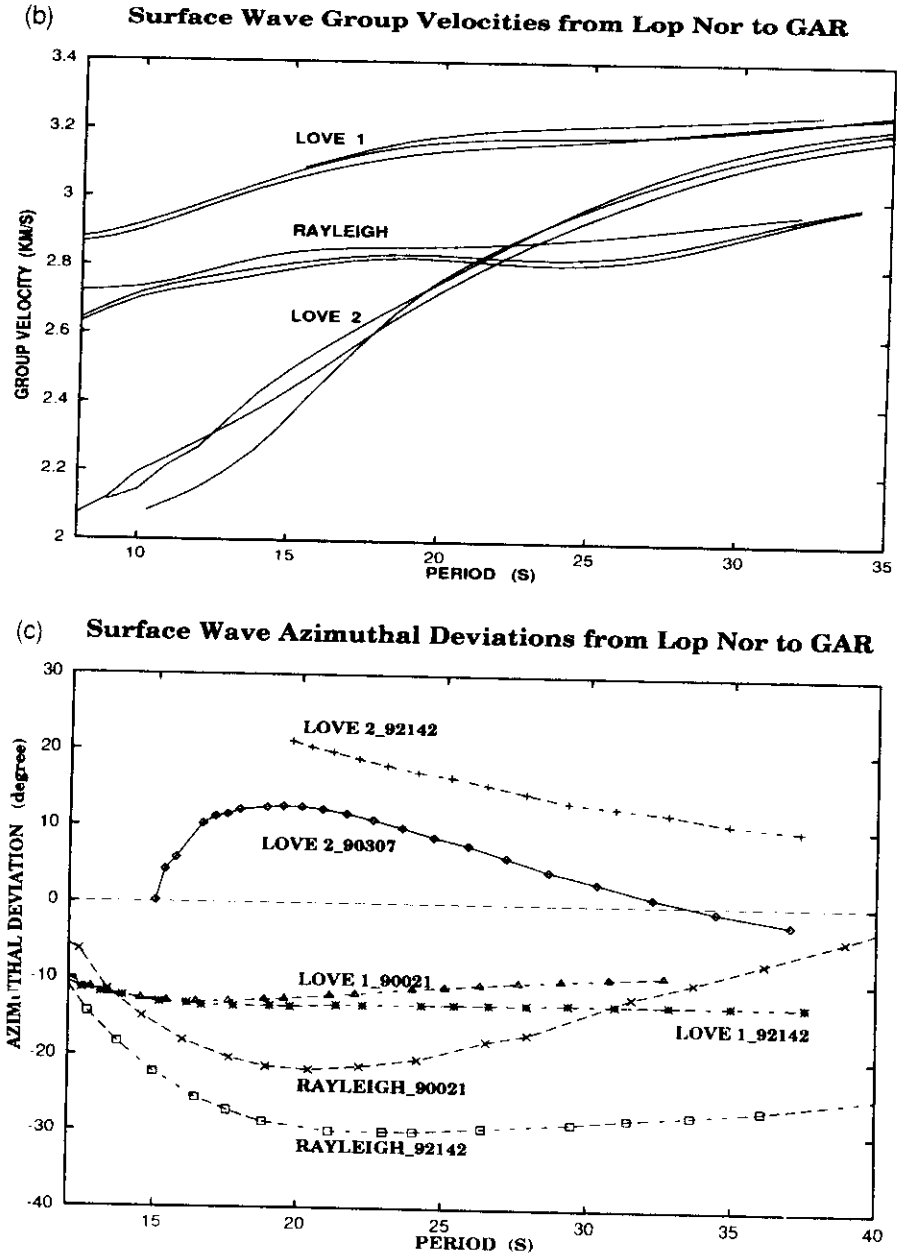

Figure 8. (*Continued.*)

vertical components shown in Fig. 9(b). Fig. 10(a) shows records of vertical, radial and transverse components for the same explosion recorded at HYB. Once again, a strong Love wave is a dominant feature of these records.

Figure 10(b) demonstrates that surface-wave group velocities observed at HYB for this explosion and for the earthquake of 1990 November 3 near Lop Nor are very similar. This implies that Love waves from the explosion are generated very close to the source and do not result from Rayleigh–Love coupling due to lateral structures along the wave path. Observations at others stations, e.g. TLY, at quite different directions from Lop Nor, and for another set of explosions and earthquakes are similar. Zhang (1994) also observed intense Love waves from the explosion on 1992 May 21 at several GSN stations (MAJO, CHTO, TATO and KEV) at greater epicentral distances than considered here.

Broad-band CDSN records of Lop Nor tests are, as a rule, not available. A single exception is the recording of the explosion on 1988 September 29 by the station WMQ (Fig. 11). At such a short distance, surface waves are only beginning to emerge, but one can see a very strong transverse component of *S* energy, indicating a highly non-isotropic source.

3 DISCUSSION

3.1 Variability of group velocities

Group velocity measurements and their interpretation in terms of lateral crustal and upper mantle structures underlying

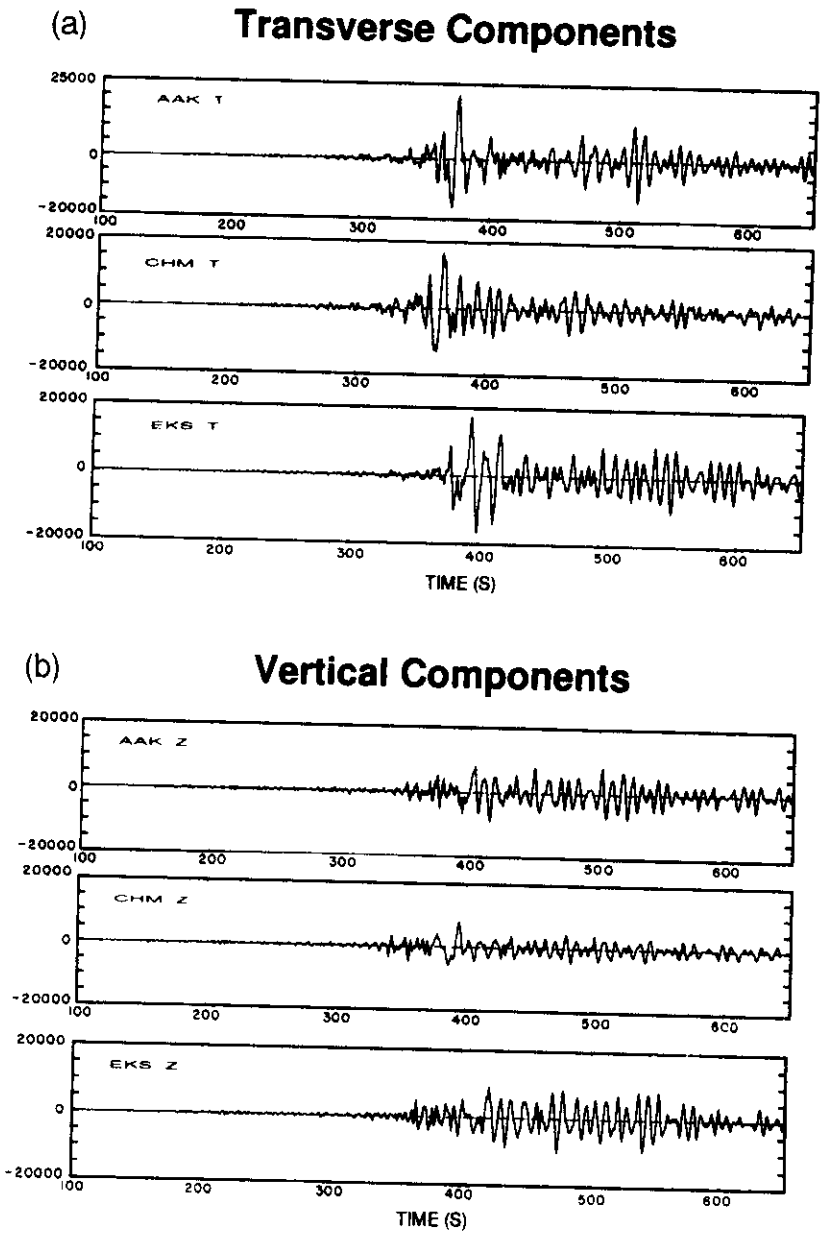

Figure 9. Comparison of (a) transverse and (b) vertical components of surface waves recorded by three KNET stations from the explosion on 1992 May 21. The high intensity of Love waves is evident.

central Asia are the focus of another study. However, it is worth noting that the features of the observed surface-wave group velocity patterns described above can be interpreted within the framework of the tectonic setting for this complex region. Paths from Lop Nor to the selected stations cross such dramatically different tectonic regimes as the Tien Shan, Pamir, Hindu Kush, Karakoram, Kunlun, Elburz, Kopet, Zagros and Himalayan Mountains, the Tibetan and Iranian plateaus, the Tarim Basin and the Indian Shield (see Fig. 1 and Table 2). The differences in surface topography along these paths are among the greatest in the world (more than 6 km for some paths) and variations in sedimentary thickness are even greater, with thicknesses ranging from more than 15 km in the eastern part of the Tarim Basin near Lop Nor to essentially zero near the Baikal Rift close to station TLY. Crustal thicknesses in the region, according to Molnar (1988), vary from 40 to 70 km.

This diversity of geological and tectonic structures crossed by the surface waves is well reflected in their group velocities and other wave characteristics. Information about group velocity variations across the region in the range of periods from 20 to 70 s may be obtained from group velocity maps in Wu & Levshin (1994) and Wu, Levshin & Kozhevnikov (1995). The group velocity curves shown on Fig. 5 complement these maps.

We qualitatively review here the cause of some of the group velocity variations observed, which are summarized in Table 2.

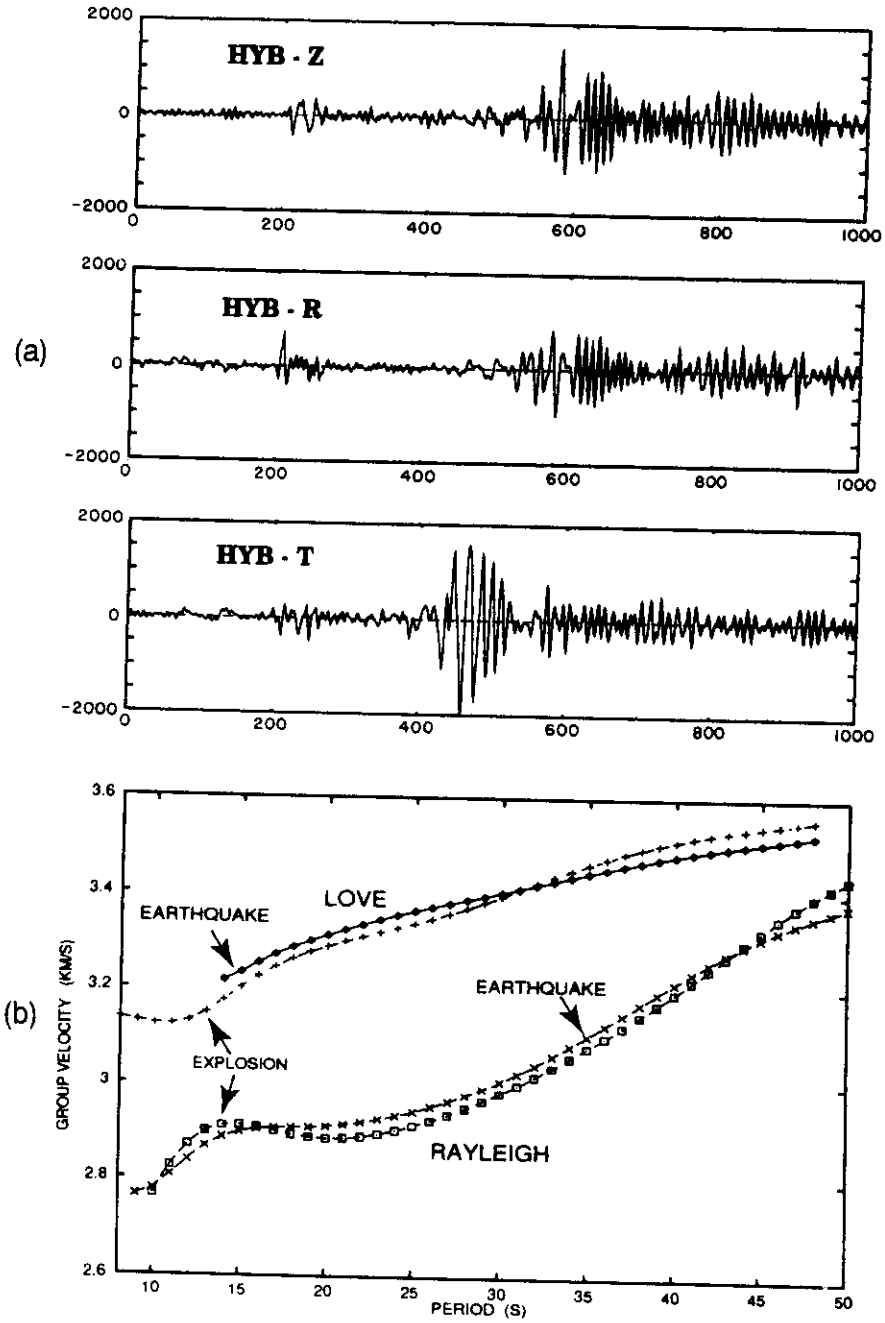

Figure 10. (a) Love waves have the highest intensity for the three-component seismogram of the explosion on 1992 May 21 recorded at HYB. (b) Group velocity curves for this event and an earthquake near Lop Nor on 1990 November 3 are very similar.

The low group velocities from Lop Nor to ABKT at short periods are due to the thick sedimentary depression stretching along the northern ridge of the Kopet mountains. Extremely low velocities along the path to LSA for periods greater than 20 s are evidently due to the very thick crust under the Tibetan plateau. Comparatively low velocities along the path to GAR may be explained by a significant thickening of the crust under the Pamir near GAR and comparatively low velocities in the upper crust in the northern part of the Tarim Basin.

Group velocity data collected as a result of this and accompanying studies can be used for tomographic inversions with a spatial resolution of the order of 200–300 km, as in the work of Wu *et al.* (1995).

3.2 Potential discriminants: surface-wave amplitude spectra and higher modes

The observations that are potentially relevant to discrimination are the following.

(1) The shapes of amplitude spectra for explosions occur-

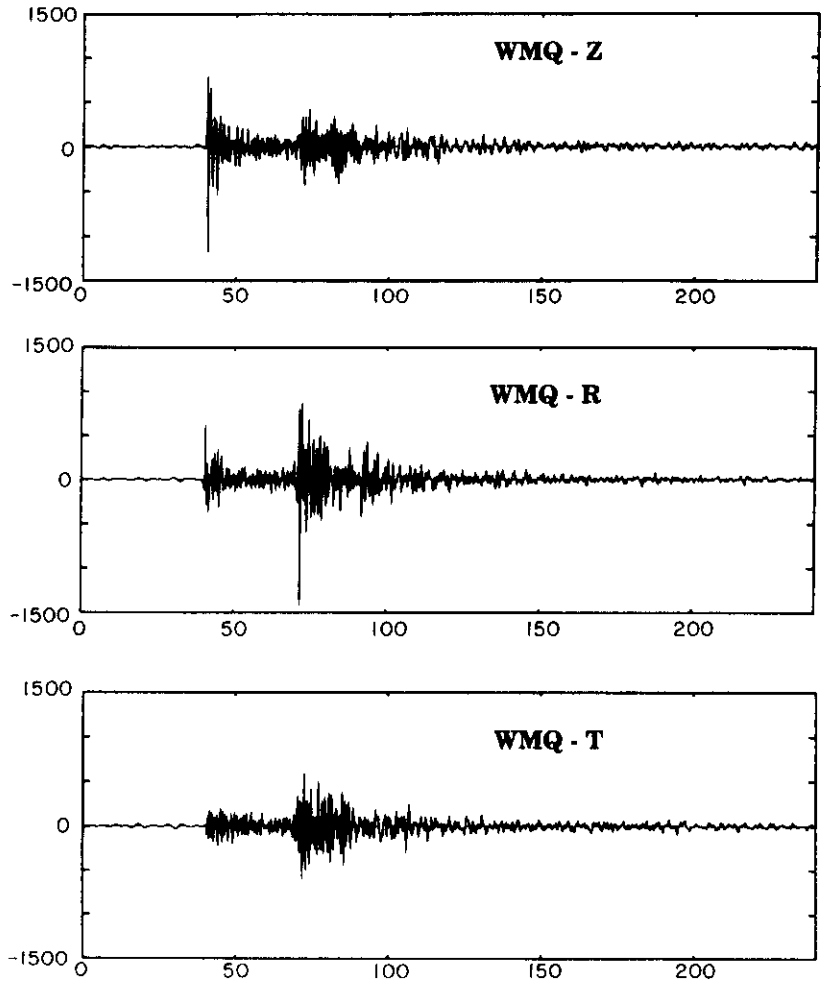

Figure 11. Strong transverse component of the *S* wave on the three-component low-passed seismogram of an explosion on 1988 September 28 recorded at WMQ.

Table 2. Characterization of wave paths from Lop Nor to selected stations.

Station	Average range (km)	Average azimuth from Lop Nor (degrees)	Main structures along the path
AAK	1200	280	Tien Shan
ABKT	2650	272	Tien Shan, Turan Platform
BJI	2305	85	E.Tarim Basin, Ala Shan Block, Ordos Platform
GAR	1600	266	E.Tarim Basin, Tien Shan
HIA	2540	60	Tarfan Basin, Altay, Mongolian Plateau
HYB	2830	201	E.Tarim Basin, Kunlun, Tibet, Himalaya, Indian Sh.
KMI	2230	140	E.Tarim Basin, Kunlun, Tibet
LSA	1310	170	E.Tarim Basin, Kunlun, Tibet
LZH	1140	110	Tarfan Basin
TLY	1589	40	Tarfan Basin, Dzhungar Basin, Altay, Sayans
WMQ	260	320	E. Tien Shan

ring at Lop Nor are nearly constant for each station, and are very similar above 10–12 s period for all of the stations of KNET.

(2) These spectra differ systematically from earthquake spectra, which are typically relatively enriched at longer periods especially for Rayleigh waves. In particular, Lop Nor explosion spectra generally peak at shorter periods and roll off faster with increasing period than for earthquakes at the same site.

(3) Higher modes are observed on Rayleigh-wave frequency–time diagrams for earthquakes, but are not observed for explosions.

These observations suggest that surface-wave spectra, in

particular Rayleigh-wave spectra, may prove useful in helping to discriminate earthquakes from explosions.

The use of surface-wave spectral amplitudes as a discriminant is complicated by one chief problem: earthquake spectra are highly variable and depend strongly on the source mechanism and wave path. It can be seen, for example, in Fig. 6(a) that both of the earthquake spectra maximize at longer periods than the explosion spectra, but the location of their spectral peaks and their roll-offs differ from one another. Although most of the earthquake spectra roll off slower with period than the explosion spectra, the spectrum for the earthquake on 1992 November 27 actually rolls off faster than any of the events at Lop Nor. Earthquake spectral variability is even greater for different paths, as Figs 6(b) and (c) indicate. This presumably is caused by propagation effects that accumulate along the wave paths through these complicated regions.

It is, therefore, unlikely that 'raw' surface-wave spectra can provide simple constraints useful for discrimination purposes. To use the information in the spectra, the raw spectrum must be supplemented with information about propagation effects so that the 'source spectrum' can be estimated. This is not a simple task, but could be accomplished either by accumulating group velocity and spectral amplitude 'master curves' or by modelling earthquake spectra by estimating detailed structural models of the crust and upper mantle underlying the region. Intermediate-period surface-wave amplitude spectra contain information of relevance to discrimination, but this information will not reveal itself in a simple phenomenological test like the m_b:M_s discriminant. It will ultimately be useful only within the framework of a systematic regional study of earthquake focal mechanisms and waves propagating in estimated 3-D regional structural models.

We have not subjected the observation of Rayleigh-wave higher modes for earthquakes to the same scrutiny applied to spectral amplitudes. However, the phenomenon is probably attributable to the fact that the earthquakes studied are deeper than the explosions and therefore excite higher modes more efficiently. The most likely use of this observation is to apply higher-mode amplitudes to produce a more accurate depth estimate, which is itself a discriminant.

3.3 Surface-wave coherence at KNET

For very weak events ($m_b < 4.0$), the measurement of spectral amplitudes at intermediate periods between 5 to 30 s using single-station records may prove impossible due to a low signal-to-noise ratio (SNR). To improve the SNR, regional networks, such as KNET, can be used as an array for stacking surface waves. The simplest means of stacking is summation of waveforms recorded at different stations with time delays corresponding to the propagation of a plane wave front with the given slowness vector across a network. A more sophisticated approach would take into account differences in phase velocities of surface waves of different periods. For the period range under consideration, such a difference may be significant. The efficiency of stacking depends on several factors, such as spatial correlation of signals and noise across a network and the accuracy of the plane wave approximation. To evaluate the range of periods within which such stacking may be efficient, we compare group velocities and amplitude spectra of Rayleigh waves extracted from KNET records from the explosion on 1992 May 21 (Fig. 7). For periods greater than 10 s, surface waves recorded at different KNET stations have very similar group-velocity and spectral-amplitude curves. For shorter periods, differences in group velocities and amplitude spectra indicate a low coherence, which implies stacking would work poorly. This conclusion is supported by results of Pavlis *et al.* (1994) and Pavlis & Mahdi (1995) who carried out stacking experiments on KNET records for several events including a Chinese nuclear test on 1994 October 7. The cut-off period, above which waves should be more nearly coherent, is dependent on the array site and the spacing of the receivers. The 10 s estimate is for KNET, with an average aperture greater than 100 km, and whose deployment covers highly variable topographic and tectonic regimes (Vernon 1994). If KNET were spatially somewhat smaller or if it were emplaced in a less structurally complex region, phase coherence would extend to shorter periods. To stack intermediate-period surface waves at KNET with periods less than 10 s will require modelling the cause of the incoherence between the stations.

3.4 Multipathing as a cause of later arrivals

The simplest explanation of the peculiar multipathing observed at GAR for different events near Lop Nor is as follows. The elongated sedimentary structure of the Eastern Tarim Basin exists south-west of Lop Nor with sedimentary thicknesses up to 16 km. Part of the shear-wave energy radiated from the source is 'trapped' by this structure which provides an efficient waveguide for Love waves propagating along the slow south-western direction. At the same time, energy radiated to the west has a tendency to refract to the north, toward the Eastern Tien Shan, where, as seen by comparing group velocity curves linking Lop Nor with AAK and Lop Nor with GAR (Fig. 6a), velocities in the crust are higher than in the Tarim Basin.

Differences in the amplitudes of the first and the second Love waves for different events may be explained by peculiarities of the radiation patterns for these events. Source mechanisms for earthquakes have been presented by Gao & Richards (1994). The event on 1990 November 3 has a strike-slip mechanism ($\theta = 310°$, $\delta = 40°$, $\lambda = -10°$) which should generate strong *SH* waves in the direction of the Tarim Basin. The earthquake on 1990 January 21 is a thrust along a near-vertical plane ($\theta = 340°$, $\delta = 78°$, $\lambda = 95°$), and *SH*-wave radiation in this direction may be poor. This is illustrated by the Fig. 12 where theoretical radiation patterns for Love and Rayleigh waves with 20 s period radiated by these two events are shown. The crustal structure model used in calculations and source mechanism estimates are taken from Gao & Richards (1994). Unfilled arrows show the direction of the great circle path to GAR. Filled arrows show the approximate direction to the eastern edge of the Tarim sedimentary basin from the epicentres of the events. We see that for an event on 1990 November 3, radiation of Love waves is near maximum in the direction of the Tarim Basin and relatively low along the great circle path. For the event on 1990 January 21, there is a node of Love-wave radiation and the maximum of radiation for Rayleigh waves in the direction to the basin. However, we do not observe a distinct slow Rayleigh wave coming from the same direction as a slow Love wave. There are several possible explanations of this fact, the most feasible of which is that for some reason Rayleigh waves are not trapped by this sedimentary basin. The other possibility is that the source mechanism

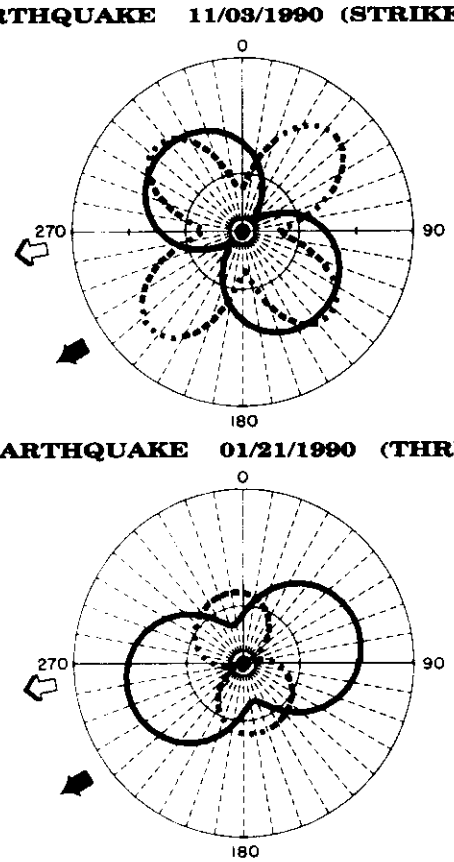

Figure 12. Theoretical radiation patterns of Love waves (dashed lines) and Rayleigh waves (solid lines) for two events (1990 November 3 and 1990 January 21) near Lop Nor at 20 s period. Filled arrows show the approximate direction from the epicentres to the eastern edge of the Tarim sedimentary basin. Unfilled arrows indicate the direction of the great circle paths to GAR.

of this event is somewhat different from that of Gao & Richards (1994).

The approach used for the interpretation of this particular strong later Love wave at GAR is a combination of group velocity and polarization measurements performed on the signal extracted by FTAN. Such a technique seems to be appropriate to study regional tectonic features (such as mountain belts, sedimentary basins, deep faults and suture zones) responsible for refraction, reflection and the trapping of surface-wave energy. Arrivals carrying this energy may, at least in some cases, be extracted from surface-wave coda and may be related to the known structural elements. This fact justifies attempts to divide the coda into two subclasses, the first of which can be interpreted deterministically, but the second one needs to be treated stochastically. Our interest is in the first subclass.

3.5 Tectonic release as an explanation for the presence of explosion-generated Love waves

The presence of a strong transverse component and well-developed Love waves generated by explosions is not unusual, especially when explosions occur in tectonically stressed regions. These phenomena are interpreted as a manifestation of co-seismic tectonic release caused by explosions in a pre-stressed medium (e.g. Press & Archambeau 1962; Brune & Pomeroy 1963; Archambeau 1972; Aki & Tsai 1972; Wallace, Helmberger & Engen 1985; Day & Stevens 1986; Day *et al.* 1987; Wallace 1991; Walter & Patton, 1991; Harkrider, Stevens & Archambeau 1994). Because the wave pattern for the earthquake of 1990 January 21, which occurred near the test site, is very similar to wave patterns of explosions (Fig. 7a), we conclude that tectonic release has a mechanism similar to the mechanism of this earthquake (thrust fault along a near-vertical plane, according Gao & Richards 1994). We should mention that Wallace (1995) suggested a strike-slip type of tectonic release for strong Lop Nor explosions. At this stage we cannot be sure of the true nature and cause of this release: either it is stress relaxation in a prestressed medium (Archambeau 1972), a near-source driven block and joint motion (Wallace *et al.* 1985; Wallace 1991, 1995), or it may be interpreted as an independent earthquake in a zone surrounding the test site triggered by the explosion (Aki & Tsai 1972). One of the possible ways to obtain a more reliable answer is a non-linear inversion for the degree 1 and 2 stress glut moments (Bukchin & Levshin 1989; Bukchin *et al.* 1994).

4 CONCLUSIONS

The primary observations made on intermediate period (5–30 s) surface waves for data accumulated in central Asia from earthquakes and nuclear explosions occurring at Lop Nor, China, are the following.

(1) Intermediate-period group-velocity measurements are highly variable across the studied region, but display understandable systematics related qualitatively to known tectonic features.

(2) These measurements, however, are repeatable in the sense that events, irrespective of type, that are physically close to one another produce similar group-velocity curves at each station.

(3) Group-velocity measurements are typically similar across KNET at periods above about 10 s, but can differ substantially across the network at shorter periods.

(4) The spectral amplitudes of nuclear explosions occurring at Lop Nor are nearly constant in shape and differ mainly in DC offset at each station.

(5) Spectral amplitudes for earthquakes on the test site are more variable, but generally are enriched at longer periods than explosions of the same magnitude, especially for Rayleigh waves.

(6) Rayleigh-wave higher modes are observed on frequency–time diagrams for earthquakes but not for the nuclear explosions.

(7) Intermediate-period waveform complexity is great; significant off-path propagation and multipathing is observed, but is related to known tectonic features.

(8) Large-amplitude Love waves are observed for the nuclear explosions at Lop Nor, indicative of significant tectonic release.

From these observations we draw the following primary conclusions.

(1) The systematics of the intermediate-period group velocity and polarization measurements forebode well for the use

of these measurements in future tomographic inversions for crustal and upper mantle structures. These models can be combined with observations of regionally propagating body waves to produce better earthquake location estimates.

(2) Intermediate-period surface-wave spectral amplitudes possess information of relevance to discrimination. However, the strong dependence of earthquake spectral amplitudes on wave path implies that 'raw' spectral amplitudes alone cannot be used as a reliable discriminant. Spectral amplitude measurements need to be interpreted to estimate the 'source spectrum'. This must be performed in the framework of a systematic regional study of earthquake focal mechanisms and waves propagating in estimated 3-D regional structural models.

(3) Careful measurements of group velocities, spectral amplitudes and polarization parameters of different surface waves, including higher modes, later arrivals and coda, may provide important information about source mechanisms and depth, as well as about tectonic features determining regional wave propagation.

(4) Surface-wave stacking above 10 s periods should effectively improve signal-to-noise ratio and reduce the surface-wave detection threshold for KNET. To stack intermediate-period surface waves with periods less than 10 s, phase incoherence between stations needs to be modelled by mapping the frequency-dependent phase-velocity variations within the network.

ACKNOWLEDGMENTS

We would like to thank Danny Harvey and Charles Archambeau for many valuable conversations. We are grateful to reviewers Gary Pavlis and Jeff Stevens for constructive comments. Ludmila Ratnikova provided a great deal of assistance in constructing figures and Daniel Quinlan provided software support. The IRIS/IDA data used in this study were acquired from IRIS's Data Management Center under the direction of Tim Ahern, the KNET data were provided by Frank Vernon, and the GEOSCOPE data were obtained from Genevieve Roult. This work was supported by a grant from IRIS and by AFOSR grants F49620-94-1-0109 and FQ8671-9500830.

REFERENCES

Aki, K. & Tsai, Y., 1972. The mechanism of Love wave excitation by explosive sources, *J. geophys. Res.*, **77**, 1452–1475.

Archambeau, C.B., 1972. The theory of stress wave radiation from explosions in prestressed media, *Geophys. J.*, **29**, 329–366.

Bakun, W.H. & Johnson, L.R., 1970. Short period spectral discriminants for explosions, *Geophys. J. R. astr. Soc.*, **22**, 139–152.

Baumgardt, D.R. & Young, G.B., 1990. Regional seismic waveform discriminants and case-based event identification using regional arrays, *Bull. seism. Soc. Am.*, **80** (Part B), 1874–1892.

Brune, J.N. & Pomeroy, P.W., 1963. Surface wave radiation patterns for underground nuclear explosions and small-magnitude earthquakes. *Bull. seism. Soc. Am.*, **68**, 5005–5028.

Bukchin, B.G. & Levshin, A.L., 1989. Estimation of earthquake focal parameters from records of surface waves in a laterally heterogeneous medium, in *Problems of Seismological Information Science*, pp. 106–114, Computational Seismology **21**, Allerton Press, NY.

Bukchin, B.G., Levshin, A.L., Ratnikova, L.I., Dost, B. & Nolet, G., 1994. An estimate of spatial–temporal characteristics of the source for Spitak earthquake using broadband digital records of surface waves, in *Computational Seismology and Geodynamics*, **2**, pp. 156–161, ed. Chowdhury, D.K. AGU, Washington, DC.

Cara, M., 1973. Filtering of dispersed wave trains, *Geophys. J. R. astr. Soc.*, **33**, 65–80.

Chael, E.P., 1988. Spectral discrimination of NTS explosions and earthquakes in the southwestern United States using high-frequency regional data, *Geophys. Res. Lett.*, **15**, 625–628.

Dahlmann, O. & Israelson, H., 1977. *Monitoring Underground Nuclear Explosions*, Elsevier, Amsterdam.

Day, S.M. & Stevens, J.L., 1986. An explanation for apparent time delays in phase-reversed Rayleigh waves from underground nuclear explosions, *Geophys. Res. Lett.*, **13**, 1423–1425.

Day, S.M., Cherry, J.T., Rimer, N. & Stevens, J.L., 1987. Nonlinear model of tectonic release from underground explosions, *Bull. seism. Soc. Am.*, **77**, 996–1016.

Dziewonski, A.M., Bloch, S. & Landisman, M., 1969. A technique for the analysis of transient seismic signals, *Bull. seism. Soc. Am.*, **59**, 427–444.

Dziewonski, A.M., Mills, J. & Bloch, S., 1972. Residual dispersion measurements: a new method of surface wave analysis, *Bull. seism. Soc. Am.*, **62**, 129–139.

Evernden, J.F., Archambeau, C.B. & Cranswick, E., 1984. An evaluation of seismic decoupling and underground nuclear test monitoring using high frequency seismic data, *Rev. Geophys.*, **24**, 143–215.

Gao, L.-P. & Richards, P.G., 1994. Studies of earthquakes on and near the Lopnor, China, nuclear test site, in *Proc. of the 16th Annual Seismic Research Symposium, 7–9 Sept. 1994*, pp. 106–112, Phillips Lab., Directorate of Geophysics.

Gutenberg, B., 1945. Amplitudes of surface waves and magnitudes of shallow earthquakes, *Bull. seism. Soc. Am.*, **35**, 3–12.

Harkrider, D.G., Stevens, J.L. & Archambeau, C.B., 1994. Theoretical Rayleigh and Love waves from an explosion in prestressed source regions, *Bull. seism. Soc. Am.*, **84**, 1410–1442.

Harjes, J.P. & Joswig, M., 1985. Signal detection by pattern recognition methods, 1985, in *The Vela Program*, pp. 579–584, ed. Kerr, A., DARPA, Washington, DC.

Harvey, D. & Hansen, R., 1994. Contributions of IRIS data to Nuclear Monitoring, *IRIS Newsletter*, **XIII**(2), 1–6.

Hedlin, A.H., Minster, J.B. & Orcutt, J.A., 1990. An automatic means to discriminate between earthquakes and quarry blasts, *Bull. seism. Soc. Am.*, **80**, 2143–2160.

Herrin, E. & Goforth, T., 1977. Phase-matched filtering: application to the study of Rayleigh waves, *Bull. seism. Soc. Am.*, **67**, 1259–1275.

Joswig, M., 1990. Pattern recognition for earthquake detection, *Bull. seism. Soc. Am.*, **90**, 170–186.

Joswig, M. & Schulte-Theis, H., 1993. Master event correlation of weak local earthquakes by dynamic waveform matching, *Geophys. J. Int.*, **113**, 562–574.

Kennett, B.L.N. 1993. The distance dependence of regional phase discriminants, *Bull. seism. Soc. Am.*, **83**, 1155–1166.

Levshin, A.L., Pisarenko, V.F. & Pogrebinsky, G.A., 1972. On a frequency–time analysis of oscillations, *Ann. Geophys.*, **28**, 211–218.

Levshin, A.L., Yanovskaya, T.B., Lander, A.V., Bukchin, B.G., Ratnikova, L.I. & Its, E.N., 1989. In *Seismic Surface Waves in a Laterally Inhomogeneous Earth*, ed. Keilis-Borok, V.I., Kluwer, Dordrecht/Boston/London.

Levshin, A.L., Ratnikova, L.I. & Berger, J., 1992. Peculiarities of surface wave propagation across the Central Eurasia, *Bull. seism. Soc. Am.*, **82**, 2464–2493.

Levshin, A.L., Ritzwoller, M.H. & Ratnikova, L.I., 1994. The nature and cause of polarization anomalies of surface waves crossing Northern and Central Eurasia, *Geophys. J. Int.*, **117**, 577–591.

Lieberman, R.C. & Pomeroy, P.W., 1969. Relative excitation of surface waves by earthquakes and underground explosions, *J. Geophys. Res.*, **74**, 1575–1590.

Molnar, P., 1988. A review of geophysical constraints on the deep structure of the Tibetan Plateau, the Himalaya and the Karakoram,

and their tectonic implications, *Phil. Trans. R. Soc. Lond.*, A, **326**, 33–88.

Murphy, J.R. & Bennett, T.J., 1982. A discrimination analysis of short-period regional seismic data recorded at the Tonto Forest Observatory, *Bull. seism. Soc. Am.*, **72**, 1351–1366.

Pavlis, G. & Mahdi, H., 1995. Surface wave propagation in Central Asia: Observations of Scattering and Multipathing with the Kyrgyz Broadband Array. *J. geophys. Res.*, submitted.

Pavlis, G., Al-Shukri, H., Mahdi, H. & Repin, D., 1994. JSP arrays and networks in Central Asia, *IRIS Newsletter*, **XIII**(2), 10–12.

Pomeroy, P.W., Best, J.W. & McEvilly, T.V., 1982. Test ban treaty verification with regional data—a review, *Bull. seism. Soc. Am.*, **72**, S89–S129.

Press, F. & Archambeau, C.B., 1962. Release of tectonic strain by underground explosions, *J. geophys. Res.*, **67**, 337–343.

Press, F., Dewart, G. & Gilman, R., 1963. A study of diagnostic techniques for identifying earthquakes, *J. geophys. Res.*, **68**, 2909–2928.

Russell, D.W., Herrman, R.B. & Hwang, H., 1988. Application of frequency-variable filters to surface wave amplitude analysis, *Bull. seism. Soc. Am.*, **78**, 339–354.

Sengor, A.M.C., Natal'in, B.A. & Burtman, V.S., 1993. Evolution of the Altaid tectonic collage and Paleozoic crustal growth in Eurasia, *Nature*, **364**, 299–307.

Stevens, J.L., 1986. Estimation of scalar moments from explosion-generated surface waves, *Bull. seism. Soc. Am.*, **76**, 123–151.

Stevens, J.L. & Day, S.M., 1985. The physical basis of m_b:M_s and variable frequency magnitude methods for earthquake/explosion discrimination, *J. Geophys. Res.*, **90**, 3009–3020.

Taylor, S.R., Sherman, N.W. & Denny, M.D., 1988. Spectral discrimination between NTS explosions and western United States earthquakes at regional distances, *Bull. seism. Soc. Am.*, **78**, 1563–1579.

Taylor, S.R., Denny, M.D., Vergino, E.S. & Glaser, R.E., 1989. Regional discrimination between NTS–explosions and earthquakes, *Bull. seism. Soc. Am.*, **79**, 1142–1176.

Terman, M., 1973. *Tectonic Map of China and Mongolia*, Geol. Soc. of Am., Boulder, Colorado.

Vernon, F., 1994. The Kyrgyz Seismic Network, *IRIS Newsletter*, **XIII**(2), 7–8.

Wallace, T.C., 1991. Body wave observations of tectonic release, in *Explosion Source Monitoring*, pp. 161–170, eds Teylor, S.T., Patton, H.J. & Richards, P.G., AGU Geophysical Monograph 65.

Wallace, T.C., 1995. S waves in seismic recordings of underground nuclear explosions, *Abstract, NATO ASI on Monitoring a Comprehensive Test Ban Treaty*, Alvor, Portugal.

Wallace, T.C., Helmberger, D.V. & Engen, G.R., 1985. Evidence of tectonic release from underground nuclear explosions in long period S waves, *Bull. seism. Soc. Am.*, **75**, 157–174.

Walter, W.R. & Patton, H.J., 1991. Tectonic release from the Soviet joint verification experiment, *Geophys. Res. Lett.*, **17**, 1517–1520.

Woods, B.B., Kedar, S. & Helmberger, D.V., 1993. M_L:M_0 as a regional seismic discriminant, *Bull. seism. Soc. Am.*, **83**, 1167–1183.

Wu, F.T. & Levshin, A.L., 1994. Surface wave tomography of China using surface waves at CDSN, *Phys. Earth planet. Inter.*, **84**, 59–77.

Wu, F.T., Levshin, A.L. & Kozhevnikov, V.M., 1995. Rayleigh wave group velocity tomography of Siberia, China and the vicinity, *Geophys. J. Int.*, in press.

Wuster, J., 1993. Discrimination of chemical explosions and earthquakes, *Bull. seism. Soc. Am.*, **83**, 1184–1212.

Zhang, J., 1994. Polarization characteristics of seismic waves from the May 21, 1992 Lop Nor nuclear explosion using IRIS/GSN broadband data, in *Proc. of the 16th Annual Seismic Research Symposium, 7–9 Sept. 1994*, pp. 393–398, Phillips Lab., Directorate of Geophysics.